Progress In Electromagnetics Research C, Vol. 47, 65–74, 2014

Reconfigurable Antenna for RFID Reader and Notched UWB Applications Using DTO Algorithm

Ahmed M. Montaser*

Abstract—In this article, the approach involving Dynamic Threshold Optimization (DTO) algorithm is considered to optimize a new compact reconfigurable antenna to be applied to triple band Radio Frequency Identification (RFID) and to ultra wideband (UWB) antenna with multiple bands notched. The antenna is implemented by using the existing techniques, such as loading an L-type band-stop filter, inserting a split ring resonator (SRR) as well as connecting L branches to the radiation disk proposed by us. In case of RFID applications, triple-band RFID 915/2450/5800 MHz are achieved separately. The results prove that this kind of antenna can be applied in RFID reader to avoid interference with other wireless systems. RF MEMS switches are used to reconfigure the antenna to be suitable for the application in the notched UWB communication systems. The DTO algorithm program is implemented using MATLAB-software and linked to the CST Microwave studio software to simulate the antenna. In addition, the optimized antenna is assessed using the Finite Difference Time Domain (FDTD) program written with MATLAB to validate the results. The experimental results for the RFID and UWB antennas show good agreement with simulated ones. The radiation patterns are satisfactorily omnidirectional across the antenna's operation bands.

1. INTRODUCTION

In the field of wireless communications, an extremely important development is the integration of different applications including cellular phones, satellite communications, RFID and wireless local area networks. Each of these applications operates at different frequency bands and requires different configurations. Due to size and complexity as well as cost constraints in designing such devices, it would be beneficial to have a reconfigurable circuitry that operates on each of these different frequencies. A reconfigurable microstrip patch antenna is an antenna which can expand the system capability by adjusting its resonant frequency, radiation pattern and polarization. Reconfigurable antennas are becoming more important in defense and commercial wireless applications.

In recent years, Radio Frequency Identification (RFID) technology has been widely used in service industries as an automatic identification tool [1]. A basic RFID system comprises a radio-scanner unit, called reader, and a set of remote transponders, denoted as tags, which include an antenna and a microchip transmitter with internal read/write memory. The tag's antenna receives signals from an RFID reader and then sends back the signals, usually including some additional data such as a unique serial number or customized information.

There are four common frequency bands have been assigned for this technology, low frequency (LF, 125–134 kHz), high frequency (HF, 13.56 MHz), ultra-high frequency (UHF, 902–928 MHz), and the so-called microwave (MW, 2.4–2.483) GHz, in addition to (5.725–5.875) GHz [1]. A low frequency operation, such as in the LF band, would suffer very slow reading in a heavily tag populated environment. Also, LF RFID requires large antenna elements and hence it is difficult to implement as well as its susceptibility to noise, which HF RFID can handle [2].

Received 12 December 2013, Accepted 11 February 2014, Scheduled 16 February 2014
* Corresponding author: Ahmed M. Montaser (Ahmed.Montaser1@techedu.sohag.edu.eg).
The author is with the Sohag University, Sohag, Egypt.

Many RFID antennas were designed to operate at one or more of the LF, HF, UHF, and MW bands and have been reported in the open literature [3–8]. The reconfigurable antenna is one of the most suitable antennas for various RFID applications. It has many advantages such as low profile, high radiation efficiency, ease of manufacturing and low fabrication cost. Each of ultra-high frequency and microwave RFID frequency bands has their own advantages, therefore, the urge of multiband RFID readers and consequently multiband reader antennas are also becoming vivid. There are few papers embraced both advantages contributed by UHF and microwave band in one patch. In [7], a triple-band printed dipole tag antenna is proposed for RFID. The triple-band printed dipole antenna is designed to operate at 0.92 GHz, 2.45 GHz and 5.8 GHz. However, the antenna size is found to be relatively large. A novel compact microstrip antenna is presented for tri-band RFID applications in [8]. The prototyped antenna showed broad impedance bandwidths (10 dB $\leq$ return loss) of 17.5, 32.7, and 25.5% accordingly in UHF (902–928 MHz), 2.45 GHz and 5.8 GHz RFID bands with stable radiation characteristics.

In this paper, the Dynamic Threshold Optimization (DTO) algorithm is considered to optimize the antenna dimensions. The DTO depends largely on Central Force Optimization (CFO), CFO algorithm had been introduced as a new deterministic metaheuristic for multidimensional search and optimization based on the metaphor of gravitational kinematics and central force optimization [9–12]. In case of the change state of switches in reconfigurable antenna, the antenna behaves as UWB antenna with multiple bands notched. This will help obtain a resonance at a lower frequency without increasing the overall antenna dimensions. Then, a dynamic technique which achieves selectivity in frequency is used [13]. This technique, known as reconfigurability, has an important switching property that allows users to access a great number of services of different frequency bands with a single wireless device [14]. Consequently, the mounting of RF switches across the U-slot would lead to a different set of resonance frequencies.

The DTO algorithm is applied to optimize the dimensions of the reconfigurable antenna to operate at 915 MHz, 2.45 GHz, and 5.8 GHz for matched input impedance (Z_{in}) of 50 Ω. The performance of the designed antenna is assessed using a full-wave EM analysis based on the Finite Difference Time Domain (FDTD) program written with MATLAB and measurement to validate the results. Finally, after connecting the RF MEMs in the specified positions in the proposed antenna, we find that the antenna behaves like a notched UWB antenna at WLAN ranges of frequencies. The paper is divided as follows. Section 2 gives a brief introduction to the dynamic threshold optimization. Section 3 explains the antenna design as well as simulation and measurement results. Finally, Section 4 presents the conclusions.

2. DYNAMIC THRESHOLD OPTIMIZATION (DTO)

Dynamic Threshold Optimization (DTO) adaptively "compresses" the decision space (DS) in a global search and optimization problem by bounding the objective function from below using auxiliary function $g(x)$ to redefine the objective function on successive DTO passes [15–17]. This approach is different from "shrinking" DS by reducing bounds on the decision variables.

DTO is conceptually quite simple. Objective function $f(x)$ is multimodal with many local maxima and a single global maximum, and the problem is to locate that maximum (coordinates and value). DTO bounds $f(x)$ from below using a series of successively increasing "thresholds," in effect compressing DS in the direction of the dependent variable (from "below") instead of, as is sometimes done, shrinking DS by reducing the independent variable's domain (from the "sides"). Locating the global maximum is easier in the compressed DS because unwanted local maxima are progressively filtered out as the "floor" (threshold) rises. Because DTO is a general geometric technique, it is algorithm-independent so that it can be used with any global search and optimization algorithm. Although DTO is described in the context of maximization, it can be applied to minimization with obvious modifications because $\max f(x) = -\min f(x)$.

Procedure OPT [$q(x)$, x^*, q^*, $q_{\min}$] is a global search and optimization routine that returns (i) the N_d coordinates x^* of a maximum of function $q(x)$, (ii) its value q^*, and (iii) a minimum value qmin(no coordinates). OPT [$\cdot$] may comprise any search and optimization algorithm (singly or in combination with others) regardless of its type, deterministic, stochastic, or hybrid; and different algorithms may be used on successive calls to OPT [$\cdot$].

DTO is initialized by applying OPT $[\cdot]$ to $f(x)$ without any threshold. Its return values then are used to define a starting threshold that subsequently is updated by applying OPT $[\cdot]$ to the auxiliary function $g(x) = [f(x) - T] \cdot U[f(x) - T] + T$, where T is the threshold value, and $U[\cdot]$ is the Unit Step function, $U(z) = \begin{cases} 1, & z \geq 0 \\ 0, & z < 0 \end{cases}$. Thus, for $f(x) > T$, $g(x) = f(x)$, whereas for $f(x) < T$, $g(x) = T$. On each successive pass, DTO changes the topology of the objective function by redefining it using auxiliary function $g(x)$. The DTO run continues until a user-specified termination criterion is met (often maximum number of passes or fitness saturation), and its pseudocode appears below:

Algorithm DTO
(i) Initialization
CALL OPT $[f(x), x_0^*, f_0^*, f_{\min}]$
Set T_0 (Starting Threshold — see text; typically $T_0 = f_{\min}$)
(ii) Loop over successive thresholds
k <— 0 (following standard notation <— means "is set to")
$F^* = -N$ (initialize best overall fitness, very large number < 0)
DO UNTIL [Termination Criterion] (see text)
(a) k <— $k + 1$ (increment pass #)
(b) Call OPT $[g(x), x_k^*, g_k^*, g_{\min}]$ where
$g(x) = [f(x) - T_{k-1}] \cdot U[f(x) - T_{k-1}] + T_{k-1}$
(c) IF $g_k^* >= F^* \therefore F^* = g_k^*$, $X^* = x_k^*$ where
X^* is the location of the best overall fitness
(d) Update Threshold: T_k (see text)
LOOP
(iii) Return: $X^*, F^* = f(X^*)$ (best overall fitness: coordinates & value)

How to set DTO's starting threshold and how it is updated are determined by the algorithm designer. One obvious starting value is the minimum fitness returned by OPT $[\cdot]$, that is, $T_0 = f_{\min}$ (which seems to be the best default choice). But updating the thresholds T_k as DTO progresses is more problematic because of the floor's profound impact on compressing DS. More and more local maxima are removed from DS as the threshold rises, so that effectively sampling DS becomes progressively more difficult (the landscape becomes flatter and flatter). In the limit of the floor rising to a global maximum, DS collapses to a plane, and there is no information available for performing a search. How well DS can be explored thus becomes more than an issue as the threshold rises, and the search algorithm's exploration characteristics become very important, Figure 1 shows the flowchart showing the main steps of the DTO algorithm.

3. ANTENNA CONFIGURATION

The geometrical structure and dimensions of the proposed printed monopole antenna are described in Figure 2. The substrate, which is 0.5 mm in thickness, is based on the low-cost FR4-epoxy material with a dielectric constant $\varepsilon_r = 4.4$. The other dimensions of the substrate are 4.2 cm for the width and 4.8 cm for the length. The ground plane is partial; a matching section connects the feed line to the patch. A 50 Ω-SMA is connected to the end of the feeding strip and grounded to the edge of the ground plane.

A split ring resonator (SRR) has been used to produce the first resonance frequency at 915 MHz. The L branches on the radiation disk are used to bring the second resonance frequency at 2.45 GHz. Finally, we use an L-type resonator coupled with the feed line to produce the third resonance frequency at 5.8 GHz. The length of $L_3 + L_4$ is about a quarter wavelength at 5.8 GHz. U-slot is used to

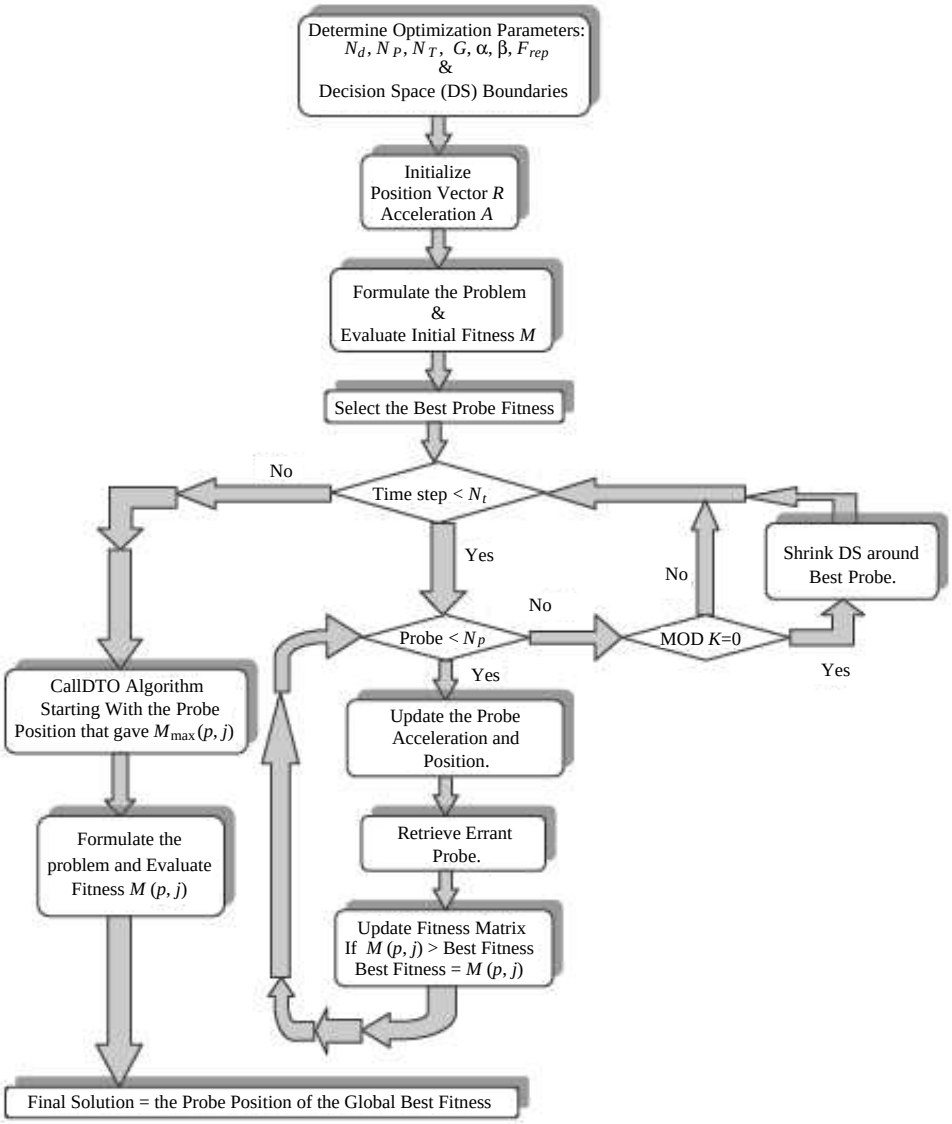

Figure 1. Flowchart showing the main steps of the DTO algorithm.

increase the antenna's electrical length for operation at lower frequency bands. A partial ground plane is considered to improve matching for different frequency bands. The geometry parameters of the antenna are $W_s = 42\,\text{mm}$, $W_L = 48\,\text{mm}$, $W_0 = 1.38\,\text{mm}$, $L_5 = 1.3\,\text{mm}$, $g_3 = 0.2\,\text{mm}$, $g_1 = 0.33\,\text{mm}$, $L_7 = 27\,\text{mm}$, $L_3 = 11.2\,\text{mm}$, $L_4 = 9.5\,\text{mm}$, $L_6 = 1\,\text{mm}$, $L_1 = 9.77\,\text{mm}$, $g_2 = 0.5\,\text{mm}$, $R_2 = 4\,\text{mm}$, $R_3 = 1\,\text{mm}$, $S_1 = 1\,\text{mm}$, $S_2 = 6\,\text{mm}$, $S_3 = 4.256\,\text{mm}$, $S_W = 3\,\text{mm}$, $R_1 = 15\,\text{mm}$, $R_4 = 8.5\,\text{mm}$, $R_0 = 15.8\,\text{mm}$, $L_8 = 18.4\,\text{mm}$, $\theta = 30^\circ$ and $\varphi = 100^\circ$. The prototype photo of the proposed antenna is shown in Figure 3.

In this paper, the proposed antenna dimensions are optimized using the DTO algorithm program. The algorithm is implemented using MATLAB-software and linked to the CST Microwave studio software to simulate the antenna. The antenna dimensions are optimized to operate at the three RFID frequency points 915 MHz, 2.45 GHz, and 5.8 GHz as center frequencies by appropriate adjustment of the antenna parameters. As a result of this study, we focus on the following antenna parameters: the length of the partial ground plane L_8, the radius of split ring resonator R_2, the length of the L branches on the radiation disk L_1, the length of rectangular slot in the patch S_2, the length of horizontal rib for L-resonator L_3, finally the length of vertical rib for L-resonator L_4.

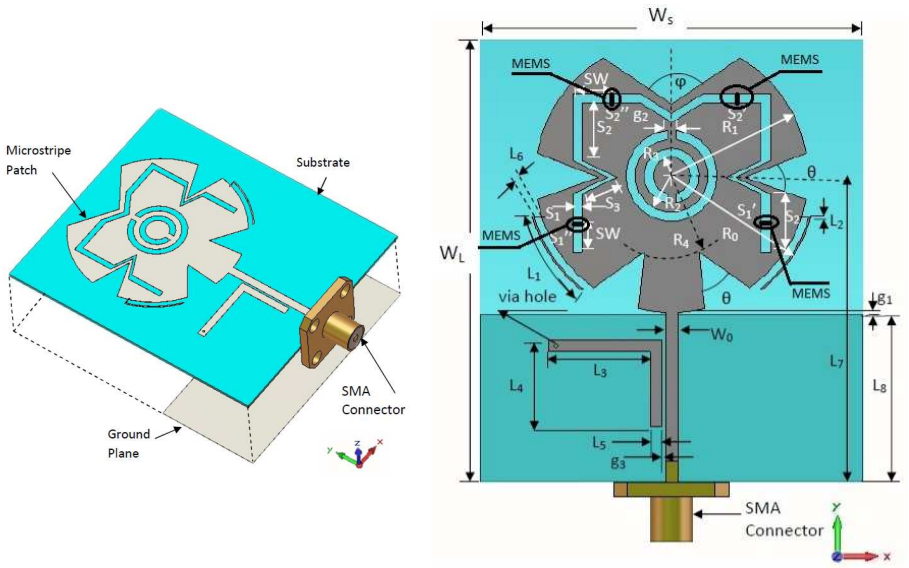

Figure 2. 3-D and 2-D for proposed antenna geometry structure.

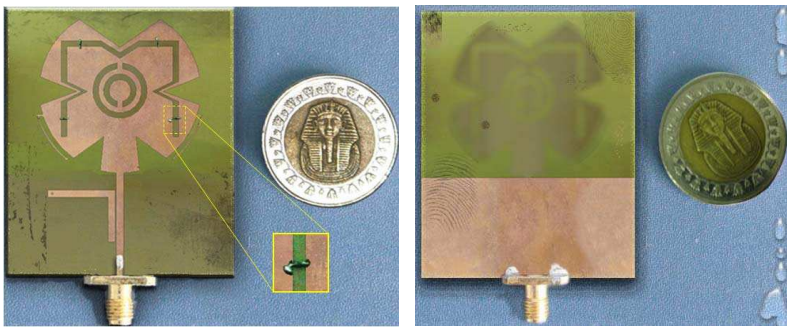

(a) (b)

Figure 3. Photograph of fabricated the antenna. (a) Top view. (b) Bottom view.

Now it is necessary to see how probes are represented in DTO algorithm. In this structure we have 6 antenna parameters (L_1, L_3, L_4, L_8, R_2 and S_2). Thus, N_d (the number of antenna parameters which are controlled by the optimization process per dimension) = 6. In the beginning, N_p probes are generated with random positions (real values) in the range of the decision space. Assuming a random acceleration assigned to each probe, the cost function or method to evaluate the goodness of a probe position is calculated. The fitness function must take the probe position and return a single number representing the value of that probe, the first step is to define the objective function focusing on the antenna return loss (S_{11}) to be less than -10 dB at the required operating bands. According to these remarks the objective function is calculated by using the following simple equation:

$$\text{Objective function} = \min(S_{11})_{(915\,\text{MHz})} + \min(S_{11})_{(2.45\,\text{GHz})} + \min(S_{11})_{(5.8\,\text{GHz})}. \quad (1)$$

By obtaining the fitness values, the new probe acceleration (the amount of change in the probe's position) can be calculated. Now it is simple to move each probe to its next position. The process is repeated until the number of time steps is finished. In this case, the resulting return loss is optimized by the CFO algorithm with 16 probe size and 80 time steps.

The optimization algorithms programmed with MATLAB will generate antenna variables which will be sent to the CST simulator for calculating the fitness value of each individual [18–20], Table 1 shows the decision space for each variable and the best obtained value to achieve our goals using DTO optimization. The optimized proposed antenna is simulated, fabricated and measured. Figure 3 shows photographs of the fabricated structure.

To validate the numerical results which have obtained from the CST simulator, the proposed antenna has been simulated by FDTD method. The parameters for FDTD computation were set as follows: the domain was $143 \times 158 \times 41$ cells with a cell size of $\Delta x = 0.41\,\text{mm}$, $\Delta y = 0.41\,\text{mm}$, $\Delta z = 0.41\,\text{mm}$. The computational domain was terminated with perfectly matched layer (PML) of 8 cells in all directions and a time step of 781.9 fs. For the CST Microwave Studio simulator, which based on the Finite Integration Technique (*FIT*), the following settings were used for time domain simulations: the minimum mesh step = 0.2, maximum mesh step = 2.05 and the mesh cells = 65,536 ($Nx = 65$, $Ny = 65$, $Nz = 17$). The mesh line ratio limit was set to 50 with an equilibrate mesh ratio of 1.19. Open add space boundary condition is applied in all directions with thermal boundaries isothermal ($T =$ constant). It is found that there are some differences between the results of EM Simulation (CST Microwave Studio based on Finite Integration Technique (FIT)) and that produced from the FDTD program written with MATLAB due to the different applied numerical techniques (FDTD and FIT). The return loss comparison between the measurements and those produced from CST Microwave Studio simulator and FDTD method are shown in Figure 4.

Parameter	Decision space	Optimized value
L_1	2–12	9.77
L_3	8–17	11.2
L_4	5–13	9.5
L_8	13–25	18.4
R_2	2–4.5	4.035
S_2	3.5–7.5	6.375

Table 1. The decision space for each variable and the best obtained value to achieve our goals using DTO optimization.

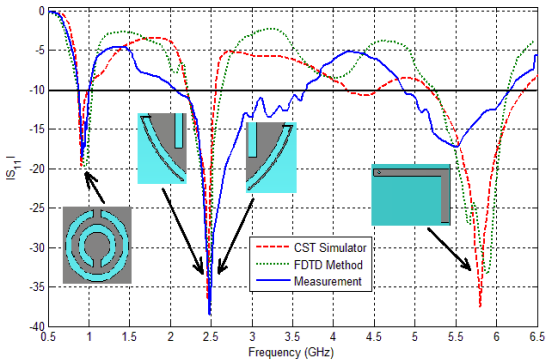

Figure 4. The return loss comparison for optimized antenna between the measurements and those produced from CST simulator and FDTD method.

Figure 5 illustrates the simulated current distribution on the optimized antenna by DTO algorithm at 915, 2450, and 5800 MHz. One can observe that most current concentrated at split ring resonator for low frequency (915 MHz) than for high frequencies (2.45 and 5.8 GHz) as shown in Figure 5(a). The electric current are mainly concentrated on the L branches on the radiation disk for middle frequency (2.45 GHz) as shown in Figure 5(b), and the L branches appears more active and the other elements of antenna appears colder at this frequency (2.45 GHz). The L-type resonator has the maximum electric current for the upper frequency (5.8 GHz) as shown in Figure 5(c). It can be concluded that the split ring resonator is responsible for generating the first band (915 MHz), the L branches on the radiation disk responsible for generating the second band (2.45 GHz), and the L-type resonator responsible for generating the third band (5.8 GHz).

The simulated radiation patterns in x-z and x-y planes of the optimized antenna at resonance frequencies of 915 MHz, 2.45 GHz, and 5.8 GHz are illustrated in Figures 6(a), 6(b) and 6(c) respectively. It is seen that the antenna gives nearly omnidirectional pattern at different operating frequencies in both planes.

The simulated and measured antenna gains for frequencies across the three bands for the proposed antenna are shown in Figure 7. The antenna gains are about 2.7–3.45 dB for the 915 MHz band, 2.4–2.9 dB for the 2.45 GHz band, and 1.3–2.55 dB for the 5.8 GHz band. For the 915 MHz and 2.45 GHz bands, the gain variations observed are less than 1 dB, respectively, while for the 5.8 GHz band, the gain variations are less than 1.5 dB. These slight differences of antenna gains can be attributed to the effects of conductor and dielectric loss. As described above, the proposed antenna has been demonstrated to basically satisfy the needs for RFID readers.

The concept of reconfigurable antennas refers to a change in the frequency characteristics of this

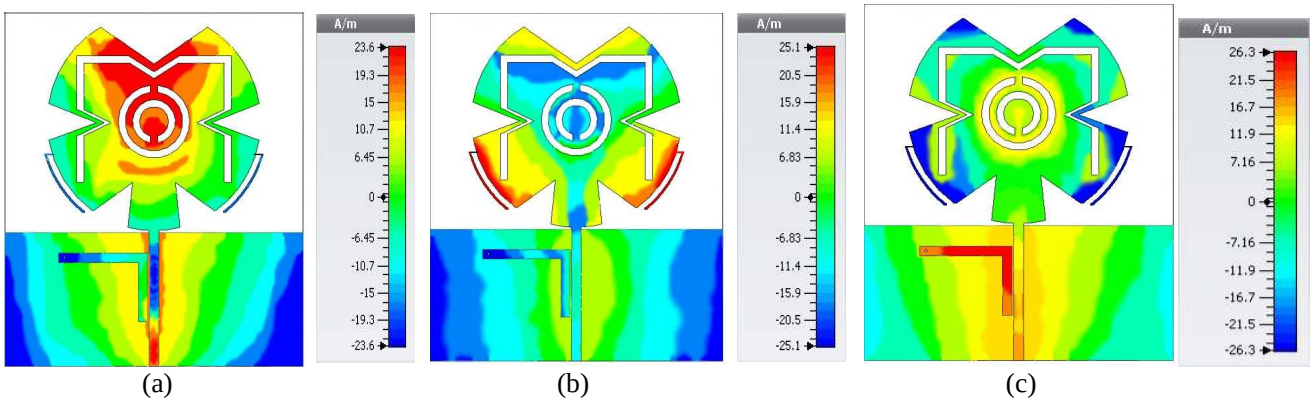

Figure 5. Simulated current distributions of the optimized antenna using DTO at different frequencies. (a) $f = 915\,\text{MHz}$, (b) $f = 2.45\,\text{GHz}$, and (c) $f = 5.8\,\text{GHz}$.

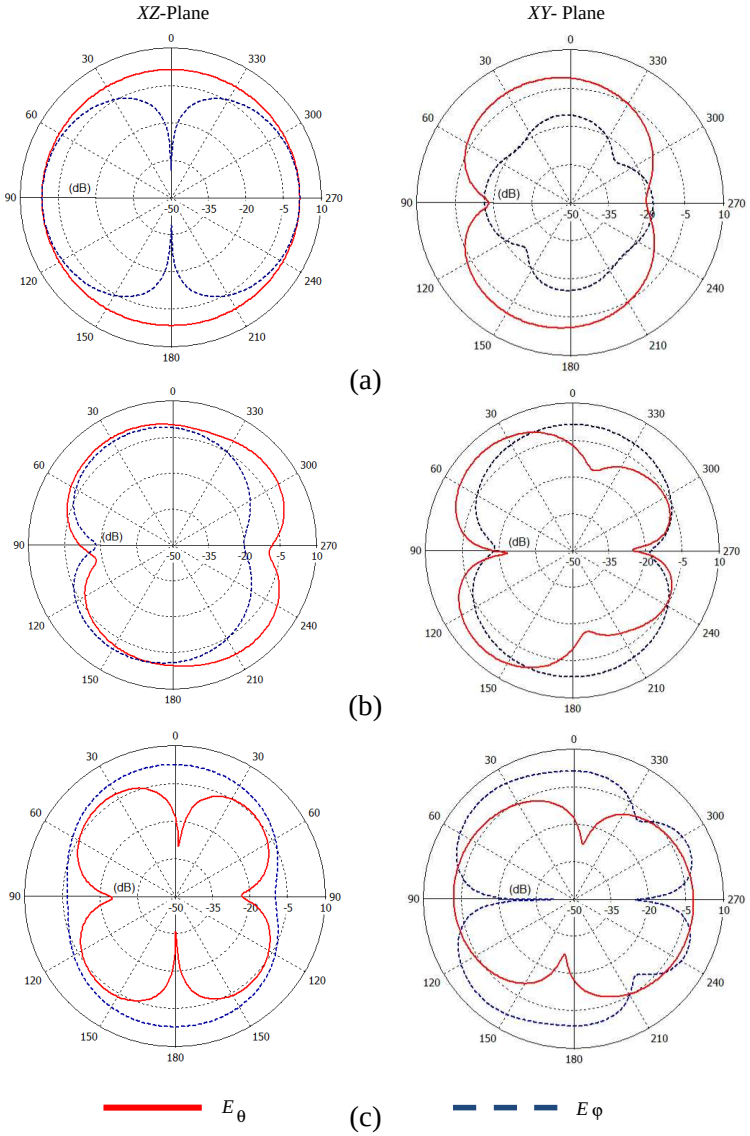

Figure 6. The radiation patterns of the proposed antenna design in xz, and xy-planes at different frequencies. (a) $f = 915\,\text{MHz}$. (b) $f = 2.45\,\text{GHz}$. (c) $f = 5.8\,\text{GHz}$.

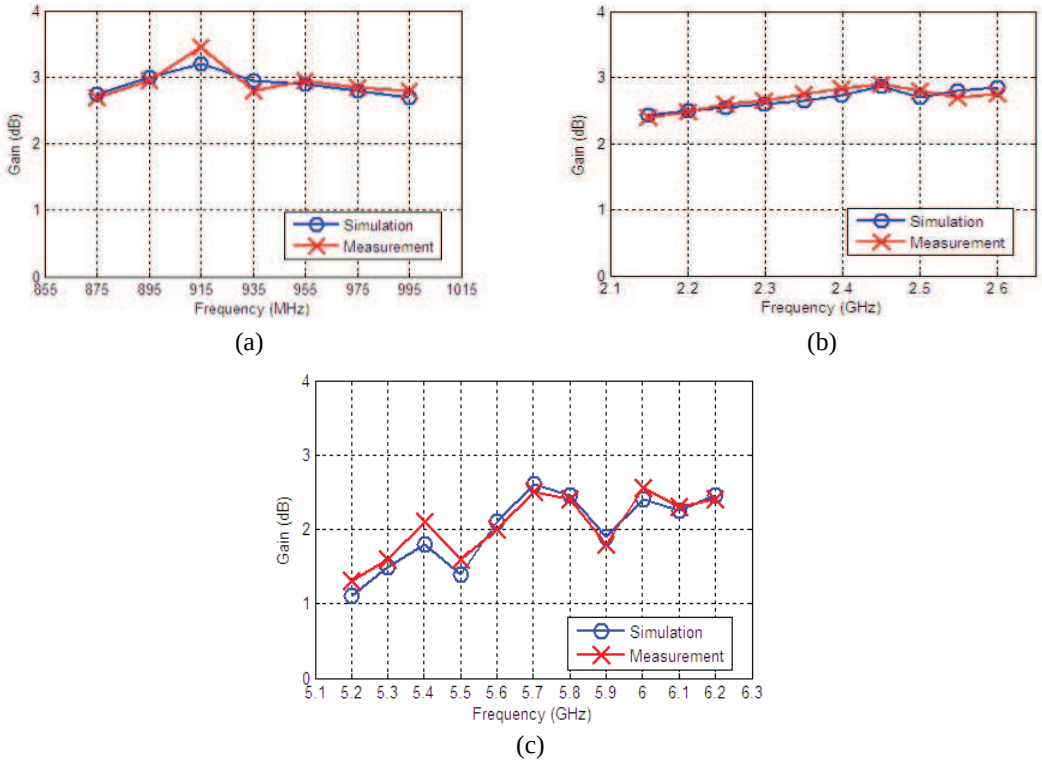

Figure 7. Simulation and Measured antenna gain for the proposed antenna. (a) Lower band at 915 MHz. (b) Middle band at 2.45 GHz. (c) Upper band at 5.8 GHz.

antenna by changing its aperture dimensions and geometry through electrical or mechanical means. Antennas with reconfigurable frequency response can either switch abruptly from a case of frequency response to another case of frequency response and continuously perform this task. Reconfigurability is achieved by mounting RF switches at selected locations across the U-slot, which is used to increase the antenna's electrical length for operation at lower frequency bands. The frequency response reconfigurability is achieved by actively controlling the effective electrical length of the antenna thus enabling the antenna to operate in different frequency bands. This is done by separating parts of the U-slot in the antenna's patch, U-slot in order to become a group of slots adjacent to each other and this in turn will affect the performance of return loss and thus the antenna will change the current distribution.

Two pairs of RF MEMS are mounted across the U slot, as indicated in Figure 2. Electrically speaking, a switch in RF systems can be represented either by a resistor to act as a short circuit or by a capacitor to act as an open circuit. Therefore, the simplest way to demonstrate an RF switch for use in this design is to construct a 400 μm × 200 μm rectangular strip that has the same dimensions of those presented in [21]. Hence, an OFF state is represented by taking this rectangular strip off the antenna, and mounting it again in the same location activates its ON state. This method for representing RF MEMS was used in [22, 23]. RF MEMS are known to possess good performance in terms of isolation and insertion loss. So, representing these by including or omitting copper strips of the same size is considered valid. However, the MEMS biasing lines are expected to slightly perturb the radiation patterns, but optimizing their locations would make the error tolerable. Figure 8 shows the effect of connecting two pairs of MEMS on the return loss of the proposed antenna, and the antenna behaves like notched UWB antenna. The measured return loss results illustrate that the reconfigurable antenna after connected two pairs of MEMS has the ability to cover a narrow resonance at GSM1900 band and UWB with a notched band cover from 2697 MHz to 5415 MHz and notched band from 5415 MHz to 5672 MHz and then back to cover after this frequency. By changing the return loss performance, this antenna can be used to notch UWB, and these notches act as filter signals interfering with the communication or

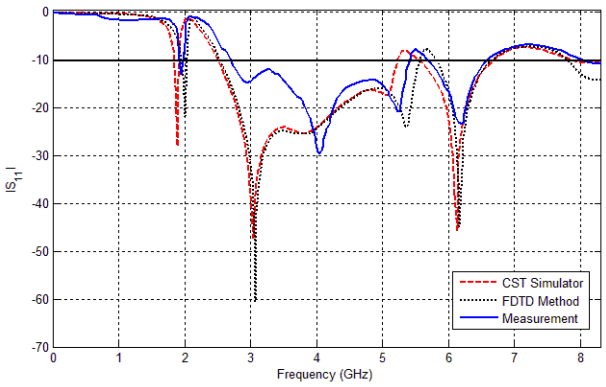

Figure 8. The return loss S_{11} for the antenna after connected two pairs of MEMS.

simply to change operating frequency band, as shown by simulated and measured return loss results in Figures 4 and 8.

The small differences between the measured and simulated return losses come from the effect of the feeding probe and SMA connector. Sometimes the input impedance for practical SMA connector is not exactly 50 ohms at high frequencies, while the simulation SMA connector is exactly 50 ohm whether in high or low frequencies.

Finally, the proposed antenna is characterized by several advantages for other multiband RFID antennas [4–8], because this antenna is more compact, with more compatibility and high gain. Moreover, this antenna is capable of reconfigurability, which gives this antenna many features and functions to help in dealing with different applications in the fields of wireless communications.

4. CONCLUSIONS

A compact reconfigurable antenna for RFID reader or notched UWB antenna application has been presented. This antenna has been designed to be electronically reconfigurable using MEMS switches. The antenna dimensions have been optimized using DTO algorithm which has been implemented in MATLAB and linked to the CST Microwave Studio simulator to simulate the antenna. The proposed antenna presents adequate matching and quite stable omnidirectional radiation patterns. These characteristics are acceptable not only for RFID systems but also for several multiband applications. Good agreement between the measurement results and both of EM Simulator CST Microwave Studio and that produced by FDTD program written with MATLAB has been achieved.

ACKNOWLEDGMENT

We would like to acknowledge the Electronics Research Institute (ERI), Microstrip Department for the support, encouragement, help and cooperation during simulation and fabrication of this research.

REFERENCES

1. Finkenzeller, K., *RFID Handbook: Radio-frequency Identification Fundamentals and Applications,* 2nd Edition, Wiley, 2004.
2. Pope, G. S., M. Y. Loukine, D. M. Hall, and P. H. Cole, "Innovative systems design for 13.56 MHz RFID," *Wireless and Portable Design Conference*, 240–245, Burlington, Massachusetts, 1997.
3. Mahmoud, K. R., "Design optimization of a bow-tie antenna for 2.45 GHz RFID readers using a hybrid BSO-NM algorithm," *Progress In Electromagnetics Research*, Vol. 100, 105–117, 2010.
4. Lu, F., Q. Feng, and S. Li, "A novel CPW-fed bow-tie slot antenna for 5.8 GHz RFID tags," *PIERS Proceedings*, 327–330, Cambridge, USA, Jul. 2–6, 2008.

5. Mayer, L. W. and A. L. Scholtz, "Dual-band HF/UHF antenna for RFID tags," *Proceeding of IEEE 68th Vehicular Technology Conference*, Vol. 21, No. 24, 1–5, Calgary, BC, Sep. 2008.
6. Yoon, J. H. and Y. C. Lee, "Modified bow-tie slot antenna for the 2.4/5.2/5.8 GHz WLAN bands with a rectangular tuning stub," *Microwave and Optical Technology Letters*, Vol. 53, No. 1, 126–130, Jan. 2011.
7. Abu, M. and M. K. A. Rahim, "Triple-band printed dipole tag antenna for RFID," *Progress In Electromagnetics Research C*, Vol. 9, 145–153, 2009.
8. Mobashsher, T., M. T. Islam, and N. Misran, "Triple band RFID reader antenna for handheld applications," *Microwave and Optical Technology Letters*, Vol. 53, No. 7, 1629–1632, Jul. 2011.
9. Formato, R. A., "Central force optimization: A new metaheuristic with application in applied electromagnetic," *Progress In Electromagnetics Research*, Vol. 77, 425–491, 2007.
10. Formato, R. A., "Central force optimization: A new gradient-like metaheuristic for multidimensional search and optimization," *Int. J. Bio-Inspired Computation*, Vol. 1, 217–238, 2009.
11. Formato, R. A., "Improved CFO algorithm for antenna optimization," *Progress In Electromagnetics Research B*, Vol. 19, 405–425, 2010.
12. Qubati, G. M., R. A. Formato, and N. I. Dib, "Antenna benchmark performance and array synthesis using central force optimization," *IET Microwaves, Antennas & Propagation*, Vol. 4, No. 5, 583–592, 2010.
13. Peroulis, D., K. Sarabandi, and L. P. B. Katehi, "Design of reconfigurable slot antennas," *IEEE Transactions on Antennas and Propagation*, Vol. 53, No. 2, 645–654, Feb. 2005.
14. Behdad, N. and K. Sarabandi, "A compact dual-/multi-band wireless LAN antenna," *IEEE Antennas and Propagation Society International Symposium*, Vol. 2B, 527–530, 2005.
15. Wang, J., "Particle swarm optimization with adaptive parameter control and opposition," *J. Computational Information Systems*, Vol. 7, No. 12, 4463–4470, 2011, http://www.jofcis.com.
16. Formato, R. A., "Parameter-free deterministic global search with simplified central force optimization," *Advanced Intelligent Computing Theories and Applications (ICIC2010), Lecture Notes in Computer Science*, Vol. 6215, 309–318, D.-S. Huang, Z. Zhao, V. Bevilacqua, and J. C. Figueroa, Eds., Springer-Verlag, Berlin, Heidelberg, 2010.
17. Hayes, B., "Quasirandom ramblings," *American Scientist Magazine*, Vol. 99, 282–287, Jul.–Aug. 2011, www.americanscientist.org.
18. Montaser, A. M., K. R. Mahmoud, A. B. Abdel-Rahman, and H. A. Elmikati, "Design Bluetooth and notched-UWB E-shape antenna using optimization techniques," *Progress In Electromagnetics Research B*, Vol. 47, 279–295, 2013.
19. Montaser, A. M., K. R. Mahmoud, and H. A. Elmikati "Design of hexa-band planar inverted-F antenna using hybrid BSO-NM algorithm for mobile phone communications," *International Journal of RF and Microwave Computer-Aided Engineering*, Vol. 23, No. 1, 99–110, Jan. 2013.
20. Montaser, A. M., K. R. Mahmoud, and H. A. Elmikati, "An interaction study between PIFAs handset antenna and a human hand-head in personal communications," *Progress In Electromagnetics Research B*, Vol. 37, 21–42, 2012.
21. Kingsley, N., D. E. Anagnostou, M. Tentzeris, and J. Papapoly-merou, "RF MEMS sequentially reconfigurable sierpinski antenna on a flexible organic substrate with novel DC-biasing technique," *Journal of Microelectromechanical Systems*, Vol. 16, No. 5, 1185–1192, Oct. 2007.
22. Costantine, J., C. G. Christodoulou, and S. E. Barbin, "A new reconfigurable multi band patch antenna," *SBMO/IEEE MTT-S International Microwave and Optoelectronics Conference, IMOC 2007*, 75–78, Oct. 29–Nov. 1, 2007.
23. Zammit, J. A. and A. Muscat, "Tunable microstrip antenna using switchable patches," *The 2008 Antennas and Propagation Conference (LAPC 2008)*, 233–236, Mar. 17–18, 2008.